Research Article

Journal of Environmental Nanotechnology

Enhancement of Efficiency and Productivity of Solar Still Using Aluminium Oxide Nanoparticles

Anitha Manisekaran[1], A. Ramalingam[2*], R. Dilip[3] and M. Dinesh Kumar[4]

[1]Department of Physics, Bharathiar University, Coimbatore, TN, India
[2]Department of Physics, Government Arts College, Udumalpet, TN, India
[3]Department of Physics, Dr. N.G.P. Arts and Science College, Coimbatore, TN, India
[4]Department of Chemistry, Dr. N.G.P. Arts and Science College, Coimbatore, TN, India
Received: 30.01.2025 Accepted: 28.02.2025 Published: 30.03.2025
*ramligri@rediffmail.com

ABSTRACT

Solar energy is an emerging field due to its, low power consumption, and renewable nature. It has a wide range of applications, including solar cells, solar panels, and solar water purifiers. Over the past decade, the scarcity of drinking water has increased globally, and in the future, the demand for fresh water is expected to rise significantly. A solar still is a simple, economical, and promising technology that converts brackish water into fresh water. However, its efficiency is limited because solar energy is only available for approximately twelve hours per day. To address this limitation, researchers are focusing on storing thermal energy using phase change materials (PCMs), which can retain excess solar energy for later use. One of the main drawbacks of passive solar stills is their low efficiency. The incorporation of phase change materials (PCMs) with aluminium oxide nanoparticles enhances productivity, especially after sunset. In this study, aluminium oxide nanoparticles were synthesized using the co-precipitation method. A passive-type solar still (single-basin, double-slope) was fabricated and tested in three different modes: i) Still without PCM ii) Still with PCM iii) Still with Nanoparticles Enhanced Phase Change Material (NPCM). The structural, morphological and thermal studies of aluminium oxide were analyzed. Various temperature parameters were recorded periodically and graphs were plotted to evaluate performance improvements.

Keywords: Solar still; Phase change material; Thermal energy storage; Al_2O_3 nanoparticle.

1. INTRODUCTION

Nanotechnology is an emerging technology which finds applications in sensors, photocatalysis, drug delivery, storage devices and in solar radiation stills (Bai and Baoxue, 2014; Sabarinathan *et al*. 2021; Bhatia, 2016; Reddy *et al.* 2012). Solar radiation is one of the best renewable sources which is used in solar cells, solar heaters and solar stills (Yin *et al*. 2014; Jamar *et al*. 2016; Elango *et al*. 2015). Water is essential for all living organisms and the quality of drinking water decreases day by day. There many methods to purify water such as, biological treatment, carbon filter, reverse osmosis process, UV radiation (Kunduru *et al*. 2017). These processes require enormous quantity of fuels. Nowadays, burning of fossil fuels poses threat to the environment. Thus, researchers focus on renewable energy sources.

Though solar stills are best in terms of water purification, the productivity rate is very less. Over the years, researchers have worked on many types of solar stills to improve their efficiency and fresh water yield by varying design and other parameters (Kaviti *et al*. 2016). The design parameters of solar stills like different shapes, different basin materials, different depths of water, heat absorbers also affect the efficiency (Ahsan *et al.* 2014). The major drawback is the availability of high radiation only for 4 hours (11 am – 2.00 pm) per day. Recently, phase change materials (PCM) have been used to maximize the utilization duration (Shanmugan *et al.* 2018). Phase change materials involve endothermic process during the day and exothermic process after sunset. So, the solar still can receive extended latent heat upto 3-4 hours. Some nanomaterials have also been reported with the properties of thermal storage and conductivity (Al *et al*. 2013). Nanoparticles when combined with PCM utilize internal heat energy from the still and improve the evaporation process.

The present work aims to investigate the effect of incorporating Al_2O_3 nanoparticles with paraffin wax (NPCM) on the efficiency and productivity of a solar still through a comparative study with only paraffin (PCM), with NPCM and without any phase change material. The Al_2O_3 nanoparticles were synthesized by co-precipitation method. The nanoparticles were characterized by XRD, FTIR, UV, PL and TEM. The thermal processes involved while using PCM and NPCM were studied by TGA.

2. MATERIALS AND SYNTHESIS METHODS

Paraffin wax and sodium dodecyl-benzene sulfonate (SDBS) was purchased from Merck, India. Aluminium oxide nanoparticles were prepared by co-precipitation method.

The research was carried out between April and May 2024. The K-type thermocouple was used to record the temperatures of water, basin, PCM tube and glass top cover in combination with a digital multi-meter (Rufuss *et al*. 2018). A pyranometer was used to measure the solar radiation. The distillate was collected in a measuring jar on hourly basis. The experiment was conducted at hourly intervals from 10:00 AM to 10:00 PM each day to record climatic parameters. The dimensions of distilled water basin still is 100 cm × 100 cm × 8 cm and the actual area of the still is 1 m^2. One-mm thick aluminium sheet was used and a black paint was coated to increase the absorption of solar radiation. Two glass plates (4 mm thick) were positioned at an inclination angle of 12° on top of the basin, aligned with the latitude to ensure optimal solar radiation exposure. The basin, measuring 113 cm × 113 cm × 20 cm, was placed inside a metal box, with sawdust filling the space between them for insulation. A 10 cm thick insulation layer was applied at the bottom, while the sides had a 5 cm thick insulation layer. To collect condensed water, channels were placed below the lower edges of the glass plates on both sides of the still, directing the fresh water into a measuring jar. Temperature measurements of the water, basin, and PCM tube were taken by inserting thermal wires into the basin's sidewalls. Insulating material was used around the insertion points to prevent heat and vapor loss.

Al_2O_3 nanoparticles were prepared using $AlCl_3$ and deionized water as precursors. In the first step, 0.2 M $AlCl_3$ was prepared using deionized water. In the second step, ammonia was added drop wise. The pH of the solution was maintained at 8. Then, the solution was stirred for 4 hours. This process was continued until the solution turned dark. In the fourth step, precipitation occurred at the end of the process, and the sample was dried at 100°C to remove any water content. The dried solution was then heated and calcined at 400°C for 3 hours, resulting in a white-coloured powder (Anitha et al., 2019).

An electronic heater was used to maintain the temperature 10°C above the melting point of paraffin wax. Sodium dodecyl benzene sulfonate was added to the paraffin in a 1:1 ratio to ensure the homogeneous dispersion of Al_2O_3 nanoparticles. Then, 0.1 wt% of Al_2O_3 nanoparticles were added. Throughout the process, the temperature was maintained at 10°C above the melting point of PCM to keep it in liquid state (Li *et al*. 2015).

3. RESULTS AND DISCUSSION

The X-ray diffraction pattern of aluminum oxide nanoparticles sintered at 900 °C is shown in Fig. 1(a). Successful preparation of the samples is confirmed by the presence of characteristic Al_2O_3 peaks, as reported in JCPDS 89-1410. The Miller indices (202), (601), (511), (220) and (114) correspond to the orientation of the monoclinic phase, indicating the formation of Al_2O_3 nanoparticles in crystallize phase (Nekouei *et al*. 2015).

Debye-Scherrer formula used for calculating the mean particle sizes of prepared sample is given below-

$$D = \frac{0.9\lambda}{\beta \cos\theta} \qquad \ldots (1)$$

where D is the crystalline size, λ (0.154 nm) represents wavelength, full width half maximum (FWHM) is measured from broadening diffraction line (β) in radians, and θ represents the Bragg reflection angle of the most intense peak in the XRD pattern (Somasundaram *et al.* 2019). The mean particle size of the prepared sample from the XRD profile was found to be 45.26 nm. The sharp and narrow peaks indicate a strong correlation with the obtained particle size. The (202) peak is the most prominent feature in the XRD pattern of the Al_2O_3 sample, representing its primary crystalline phase.

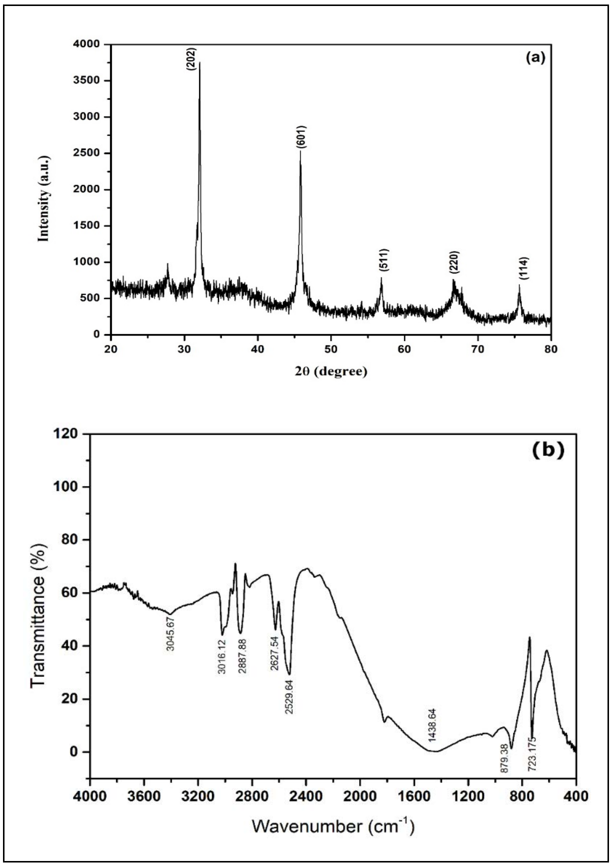

Fig. 1: (a)X-ray diffraction pattern and (b) FTIR spectrum of Al_2O_3 nanoparticles

Al_2O_3 nanoparticles are characterized by their average particle size and morphology, making them suitable for use as a thermal energy storage medium. The measured particle size of Al_2O_3 is less than 100 nm, confirming its classification as a nanoparticle. The co-precipitation process effectively controls the small crystalline size of Al_2O_3 nanoparticles while also enhancing their crystallinity.

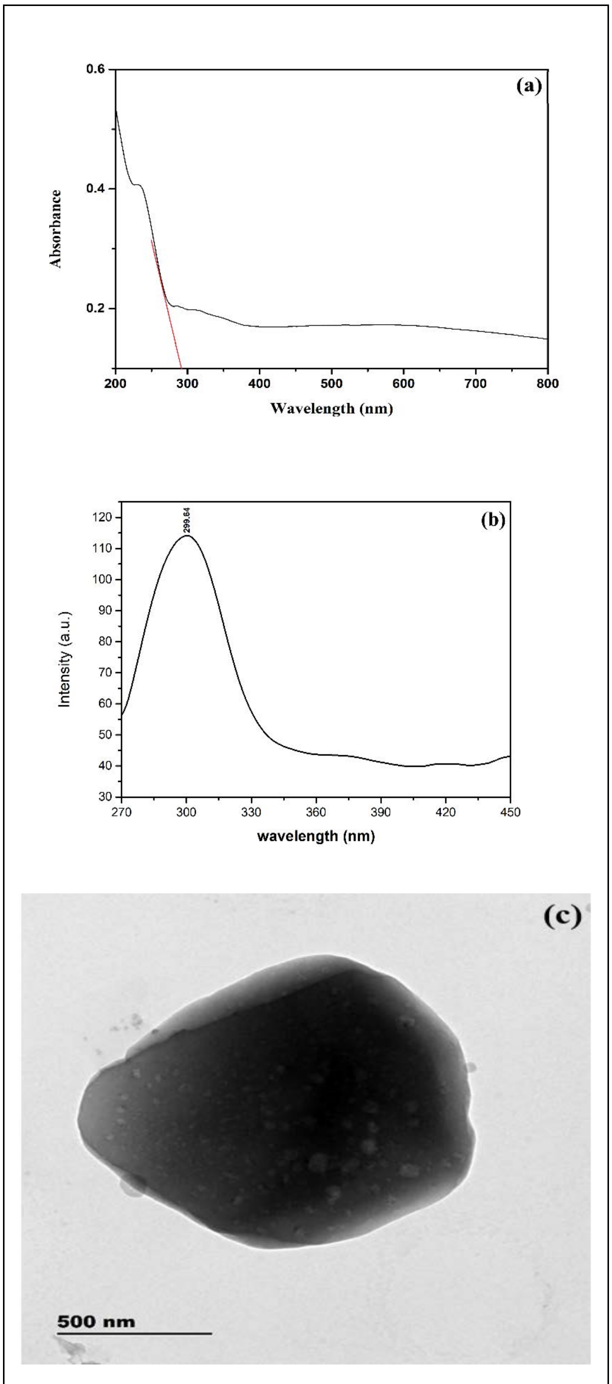

Fig. 2: (a) UV-Visible Spectroscopy, (b) PL and (c) TEM patterns of Al_2O_3 nanoparticles

The FT-IR spectrum of Al_2O_3 nanoparticles, recorded in the 4000–400 cm^{-1} range, is shown in Fig. 1(b). The peak at 1438.64 cm^{-1} corresponds to –OH vibration, while the peaks at 723.175 cm^{-1} and 879.38 cm^{-1} represent Al–O vibrations (Mozgawa, 2000). Additionally, peaks observed at 3016.12 cm^{-1}, 2887.88 cm^{-1}, and 2627.54 cm^{-1} correspond to the stretching vibrations of O–H, C–H, and C=O groups, respectively (Devi and Gayathri, 2010). The FT-IR spectrum confirms that the Al_2O_3 nanoparticles exhibit all major characteristic peaks, aligning well with a literature study (Miao *et al*. 2019).

Fig. 2(a) illustrates the UV-visible spectrum of Al_2O_3 nanoparticles. The spectrum shows a narrow band at a wavelength of 283 nm, which is consistent with the material's high refractive index and brightness. The photoluminescence spectrum of Al_2O_3 nanoparticles recorded at room temperature is shown in Fig. 2(b). The excitation peak is centered at 299.64 nm, indicating violet emission. The assigned peak intensity of the curve for Al_2O_3 nanoparticles is 114.52 a.u. This observation suggests that aluminium oxide may induce the intersystem crossing. The appearance of single band emission at 299.64 nm for the samples indicates good crystallinity of the Al_2O_3 nanoparticles.

Fig.2(c) shows the TEM image of Al_2O_3 nanoparticles synthesized using co-precipitation method. The TEM image exhibits magnified view of the prepared sample, clearly displaying spherical-shaped particles. The spherical morphology offers a large surface area, which could positively impact the material's thermal storage (Li *et al.* 2020).

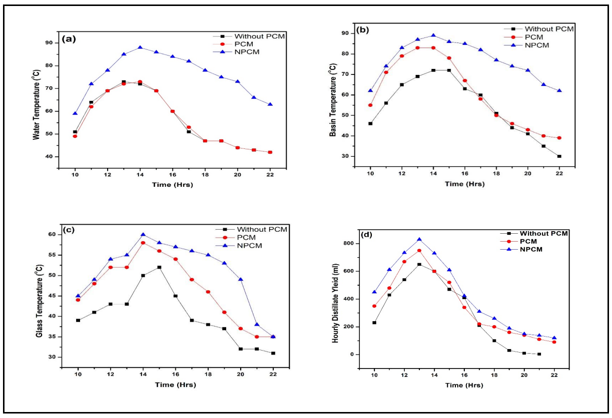

Fig. 3: Hourly variation of water, basin, glass temperature and distillate yield with respect to time of solar still without PCM, PCM and NPCM

A thermometer was used to measure ambient temperature and wind velocity was measured with an electronic anemometer. Fig. 3 depicts a comparative analysis of three different solar still configurations namely, without PCM, with PCM and with NPCM. Fig. 3(a) shows the water temperature variation over time for the three modes. The maximum water temperatures recorded were 72°C, 74°C and 88°C, respectively, at 2.00 PM. However, after sunset, the water temperature in the solar still without PCM dropped rapidly. In contrast, the PCM and NPCM-integrated stills exhibited better thermal retention, preventing the temperature from rapidly decreasing to room temperature. The variation of basin and glass temperatures over time are shown in Fig. 3(b) and (c).

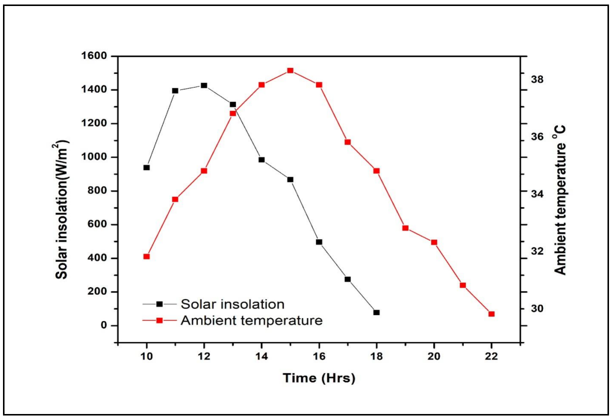

Fig. 4: Variation of solar insolation and ambient temperature with respect to time

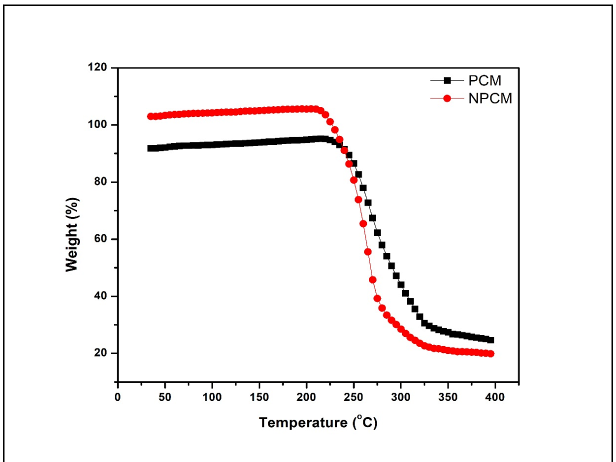

Fig. 5: Thermogravimetric curves for PCM and NPCM

Fig. 3(d) depicts the hourly distillate yield in mL for three modes of solar still. The still without PCM produced 3680 mL/m^2/day whereas the still with PCM tubes produced an output of 4690 mL/m^2/day and still with NPCM tubes produced a distillate output of 5327 mL/m^2/day. The maximum yield was attained by the still with NPCM at 2.00 PM. The still without PCM collected less than 100 mL of desalinated water by 5.00 PM. The latent heat released by NPCM was more than PCM due to the influence of spherical shaped aluminium oxide nanoparticles. The fresh water collected by the PCM still dropped below 100 mL by 8:00 PM, while the NPCM still reached this level by 11:00 PM. The temperature of the system without PCM drops rapidly after 3:00 PM. However, in the cases of PCM and NPCM, the temperature decreases more gradually. Regarding productivity yield, there is a significant difference of approximately 1000 mL between the PCM and non-PCM modes.

The variation of ambient temperature and solar insolation over time is presented in Fig. 4. The ambient temperature was observed to range between 30°C and 38.5°C, while the maximum solar insolation reached 1526 W/m^2.

The PCM and NPCM systems each collected around 637 mL of desalinated water. The results clearly indicate that nanoparticles enhance thermal conductivity and latent heat storage in the solar still. Thermogravimetric analysis was conducted on PCM and NPCM samples by heating them from 30°C to 400°C at a rate of 10 °C/min. The TG curves show weight loss as a function of temperature. An endothermic peak was observed as the temperature increased between 30°Cand 150°C, demonstrating that NPCM absorbed more latent heat than PCM (Fig. 5). An exothermic peak was detected in the range 212–325°C for NPCM and 240–320°C for PCM, indicating that NPCM released more heat than PCM. The decomposition effect, associated with mass loss, was measured at 24.6% for PCM and 19.7% for NPCM.

4. CONCLUSION

The performance of solar still without PCM, PCM and NPCM was investigated in this report. The distilled water collected without PCM, PCM and NPCM are 3680, 4690 and 5327 mL/m^2/day, respectively. The thermal storage of still with PCMs and NPCM can play a significant role, which is linked with latent heat of PCM. Solar still with NPCM enhanced the productivity about 28% compared with PCM. The TG analysis also supports that NPCM performed better than PCM.

DATA AVAILABILITY STATEMENT

The data used to support the findings of this study are included within the article.

CREDIT AUTHOR STATEMENT

Anitha Manisekaran: Writing - original draft, Data curation. **A. Ramalingam**: Formal analysis. **M. Dinesh Kumar:** Conceptualization, Software. **R. Dilip**: Investigation, Methodology, Validation.

CONFLICTS OF INTEREST

The authors declare that there is no conflict of interest.

FUNDING

This research received no specific grant from any funding agency in the public, commercial, or not-for-profit sectors.

REFERENCES

Ahsan, A., Imteaz, M., Thomas, U. A., Azmi, M., Rahman, A. and Daud, N. N. N., Parameters affecting the performance of a low cost solar still, *Appl. Energy*, 114, 924-930(2014). https://doi.org/10.1016/j.apenergy.2013.08.066

Al, K., Hussain, H., Saw, C. L. and Afolabi, L., Review on nanomaterials for thermal energy storage technologies, *Nanosci. Nanotechnol*., 3(1), 60-71(2013). https://doi.org/10.2174/22113525113119990011

Anitha, M., Ramalingam, A. and Jayaprakash, R., Productivity Enhancement of a Single Basin Double slope Solar Still Coupled with PCM Tubes, J. eng. Res. Appl., 9(6), 01-06(2019). https://doi.org/10.1080/19443994.2014.1003973

Bai, J. and Baoxue, Z., Titanium dioxide nanomaterials for sensor applications, *Chem. Rev.,* 114(19), 10131-10176(2014). https://doi.org/10.1021/cr400625j

Bhatia, S., Nanoparticles types, classification, characterization, fabrication methods and drug delivery applications, *Nat. polym. drug delivery syst.,* 33-93(2016). https://doi.org/10.1007/978-3-319-41129-3_2

Devi, T. S. R. and Gayathri, S., FTIR and FT-Raman spectral analysis of paclitaxel drugs, *Int. J. Pharm. Sci. Rev. Res.,* 2(2), 106-110(2010).

Elango, T., Kannan, A. and Kalidasa, K. M., Performance study on single basin single slope solar still with different water nanofluids, *Desalin.*, 360, 45-51(2015). https://doi.org/10.1016/j.desal.2015.01.004

Jamar, A., Majid, Z. A. A., Azmi, W. H., Norhafana, M. and Razak, A. A., A review of water heating system for solar energy applications, *Int. Commun. Heat Mass Transfer,* 76, 178-187(2016). https://doi.org/10.1016/j.icheatmasstransfer.2016.05.028

Kaviti, A. K., Yadav, A. and Shukla, A., Inclined solar still designs, *Renewable Sustainable Energy Rev.,* 54, 429–451(2016). https://doi.org/10.1016/j.rser.2015.10.027

Kunduru, K. R., Michael, N., Shady, F., Rajendra, P. P., Arijith, B. and Abraham, J. D., Nanotechnology for water purification: applications of nanotechnology methods in wastewater treatment, *Water Purif.*, 33-74(2017). https://doi.org/10.1016/B978-0-12-804300-4.00002-2

Li, L. Mao, D., Jun, Y. and Xiaoming, G., Highly selective hydrogenation of CO2 to methanol over CuO–ZnO–ZrO2 catalysts prepared by a surfactant-assisted co-precipitation method, *J. Power Sources,* 279 394-404(2015). https://doi.org/10.1016/j.jpowsour.2014.12.142

Li, D., Ruidong, X., Tian, M., Jia, Y., Zhenhua, G., Xing, Z. and Kongzhai, L., Encapsulated Co3O4/(SiAl@Al2O3) thermal storage functional catalysts for catalytic combustion of lean methane, *Appl. Therm. Eng.,* 181, 116012(2020). https://doi.org/10.1016/j.applthermaleng.2020.116012

Miao, W., Wang, Y., Li, X., Shulie, G., Yang, L. and Zhuolin, L., Development of spherical α-Al2O3-based composite phase change materials (PCMs) and its utilization in thermal storage building materials, *Thermochim. Acta*., 676, 177-185(2019). https://doi.org/10.1016/j.tca.2019.04.010

Mozgawa, W., The influence of some heavy metals cations on the FTIR spectra of zeolites, *J. Mol. Struct.,* 555(1-3), 299-304(2000). https://doi.org/10.1016/S0022-2860(00)00613-X

Nekouei, F., Shahram, N., Tyagi, I. and Vinod, K. G., Kinetic, thermodynamic and isotherm studies for acid blue 129 removal from liquids using copper oxide nanoparticle-modified activated carbon as a novel adsorbent, *J. Mol. Liq*., 201, 124-133(2015). https://doi.org/10.1016/j.molliq.2014.09.027

Reddy, A. L. M., Sanketh, R. G., Shaijiumon, M. M. and Ajayan, P. M., Hybrid nanostructures for energy storage applications, *Adv. Mater.,* 24(37), 5045-5064(2012). https://doi.org/10.1002/adma.201104502

Rufuss, D. D. W., Suganthi, L., Iniyan, S. and Davies, P. A., Effects of nanoparticle-enhanced phase change material (NPCM) on solar still productivity, *J. Cleaner Prod.*, 192 9-29(2018). https://doi.org/10.1016/j.jclepro.2018.04.201

Sabarinathan, A., Jayaprakash, R., Gopi, S. and Robert, R., The Augmentation of Photocatalytic Efficiency Due to the Transition Effect Between Spherical Shape and Rod-Like Structure of Sn Levels in ZnO Nanoparticles, *J. Inorg. Organomet. Polym. Mater.,* 31(4), 1480-1490(2021). https://doi.org/10.1007/s10904-020-01769-2

Shanmugan, S., Palani, S. and Janarthanan, B., Productivity enhancement of solar still by PCM and Nanoparticles miscellaneous basin absorbing materials, *Desalin*, 433 186-198(2018). https://doi.org/10.1016/j.desal.2017.11.045

Somasundaram, G., Jayaprakash, R., Sangaiya, P. and Dilip, R., Phytochemicals and morphological influence of aloe barbadensis miller extract capped biosynthesis of CdO nanosticks, *J. Inorg. Organomet. Polym. Mater.,* 29(6), 1862-1873(2019). https://doi.org/10.1007/s10904-019-01147-7

Yin, Z., Jixin, Z., Qiyuan, H., Xiehong, C., Chaoliang, T., Hongyu, C., Qingyu, Y. and Hua, Z., Graphene-based materials for solar cell applications, *Adv. energy mater*., 4(1), 1300574(2014). https://doi.org/10.1002/aenm.201300574